The small-molecule VEGF receptor inhibitor pazopanib (GW786034B) targets both tumor and endothelial cells in multiple myeloma

Klaus Podar*†, Giovanni Tonon*, Martin Sattler*, Yu-Tzu Tai*, Steven LeGouill*‡, Hiroshi Yasui*, Kenji Ishitsuka*, Shaji Kumar§, Rakesh Kumar¶, Lini N. Pandite¶, Teru Hideshima*, Dharminder Chauhan*, and Kenneth C. Anderson*†

*Department of Medical Oncology, Dana–Farber Cancer Institute, Harvard Medical School, Boston, MA 02115; ‡Institut National de la Santé et de la Recherche Médicale U0601, Institut de Biologie and Service d'Hématologie Clinique, Hôtel-Dieu Centre Hospitalier Universitaire de Nantes, 44093 Nantes, France; §Division of Hematology, Mayo Clinic, Rochester, MN 55905; and ¶GlaxoSmithKline, Research Triangle Park, NC 27709

Communicated by Judah Folkman, Harvard Medical School, Boston, MA, October 23, 2006 (received for review December 15, 2005)

A critical role for vascular endothelial factor (VEGF) has been demonstrated in multiple myeloma (MM) pathogenesis. Here, we characterized the effect of the small-molecule VEGF receptor inhibitor pazopanib on MM cells in the bone marrow milieu. Pazopanib inhibits VEGF-triggered signaling pathways in both tumor and endothelial cells, thereby blocking *in vitro* MM cell growth, survival, and migration, and inhibits VEGF-induced up-regulation of adhesion molecules on both endothelial and tumor cells, thereby abrogating endothelial cell-MM cell binding and associated cell proliferation. We show that pazopanib is the first-in-class VEGF receptor inhibitor to inhibit *in vivo* tumor cell growth associated with increased MM cell apoptosis, decreased angiogenesis, and prolonged survival in a mouse xenograft model of human MM. Low-dose pazopanib demonstrates synergistic cytotoxicity with conventional (melphalan) and novel (bortezomib and immunomodulatory drugs) therapies. Finally, gene expression and signaling network analysis show transcriptional changes of several cancer-related genes, in particular c-Myc. Using siRNA, we confirm the role of c-Myc in VEGF production and secretion, as well as angiogenesis. These preclinical studies provide the rationale for clinical evaluation of pazopanib, alone and in combination with conventional and novel therapies, to increase efficacy, overcome drug resistance, reduce toxicity, and improve patient outcome in MM.

angiogenesis | xenograft mouse model

In solid tumors, angiogenesis is closely related to tumor growth and metastatic potential. In addition, recent studies also suggest a role for angiogenesis in hematologic malignancies, including multiple myeloma (MM). Therefore, targeting angiogenesis is a potentially potent approach in cancer treatment (1–3). Vascular endothelial growth factor (VEGF) (4) is present in the bone marrow (BM) microenvironment of patients with MM and associated with angiogenesis. The extent of angiogenesis has been correlated directly with plasma-cell proliferation and labeling index and is inversely related with patient survival (5). Previous studies showed that VEGF is expressed and secreted by MM cells and BM stromal cells and, in turn, stimulates IL-6 secretion by BM stromal cells, thereby augmenting paracrine MM cell growth. Moreover, IL-6 enhances the production and secretion of VEGF by MM cells. VEGF and VEGFR-1 (Flt-1) are coexpressed in both MM cell lines and patient MM cells, and VEGF-triggered effects in MM cells are mediated via Flt-1. Importantly, binding of VEGF increases MM cell growth, survival, and migration, thereby demonstrating the crucial role of VEGF in MM cell pathogenesis in the BM milieu (3).

A recent milestone in cancer therapy was the approval of the humanized monoclonal antibody against VEGF, bevacizumab (Avastin), by the U.S. Food and Drug Administration as a first-line therapy for metastatic colorectal cancer in February 2004. Bevacizumab represents the first cancer drug specifically designed to target VEGF and, thereby, inhibit tumor angiogenesis. Subsequent studies have demonstrated the effectiveness of bevacizumab in several other tumors, including non-small cell lung cancer, breast cancer, pancreatic cancer, melanoma, and metastatic renal-cell cancer, but only when combined with conventional chemotherapy (3, 6). Besides bevacizumab, which is administered intravenously, many other VEGF inhibitors have been developed. Based upon their bioavailability profile, several VEGF receptor inhibitors were developed as small-molecule receptor tyrosine kinase inhibitors. In marked contrast to bevacizumab, small-molecule antiangiogenic receptor tyrosine kinase inhibitors including PTK/ZK222584 (7) have failed to mirror its chemosensitizing ability. Only recently have encouraging results for second-generation antiangiogenesis drugs including sorafenib (Bayer, West Haven, CT) and sutent (Pfizer, New York, NY) been reported in solid tumors (7), and to date, their clinical efficacy in hematologic malignancies, including MM, is undefined.

Our and other prior studies have evaluated several first-generation small-molecule VEGF receptor inhibitors for their therapeutic activity in MM, including the receptor tyrosine kinase inhibitor PTK787/ZK222584 (Novartis Pharma, Basel, Switzerland) and the pan inhibitor of VEGF receptors GW654652 (GlaxoSmithKline). These VEGF receptor inhibitors showed significant anti-MM efficacy *in vitro* (3).

Pazopanib (GW786034B; GlaxoSmithKline) is a novel orally available, small-molecule tyrosine kinase inhibitor of VEGF receptor -1, -2, and -3 with IC_{50} values of 10, 30, and 47 nM, respectively (‖, 8). An initial nonrandomized, dose-escalation phase I study with pazopanib (GSK-VEG10003) showed stable disease or partial responses in relapsed/refractory patients with renal cell (RCC), Hurthle cell, neuroendocrine, GIST, adeno lung carcinoma, chondrosarcoma, leiomyosarcoma, and melanoma. Remarkably, of 12 patients with RCC, 7 patients had stable disease or tumor reduction and 1 patient had a partial response. Adverse side effects included manageable hypertension, tiredness and hair depigmentation (9). Based on this study, several clinical studies are ongoing, including

Author contributions: K.P., G.T., and M.S. designed research; K.P., S.L., H.Y., K.I., S.K., and R.K. performed research; R.K. and L.N.P. contributed new reagents/analytic tools; K.P., G.T., M.S., Y.-T.T., T.H., D.C., and K.C.A. analyzed data; and K.P. and K.C.A. wrote the paper.

Conflict of interest statement: R.K. and L.N.P. are employees of GlaxoSmithKline, Research Triangle Park, NC.

Abbreviations: BM, bone marrow; Dox, doxorubicin; HUVEC, human umbilical endothelial cell; MM, multiple myeloma.

†To whom correspondence may be addressed. E-mail: klaus_podar@dfci.harvard.edu or kenneth_anderson@dfci.harvard.edu.

‖Kumar, R. Knick, V. B., Rudolph, S. K., Johnson, J. H., Crosby, R. M., Hopper, T. M., Miller, C. G., Onori, J. A., Mullin, R. J., *et al.* (2005) AACR-NCI-EORTC International Conference on Molecular Targets and Cancer Therapeutics, November 14–18, 2005, Philadelphia, PA, pp 58–59.

This article contains supporting information online at www.pnas.org/cgi/content/full/0609329103/DC1.

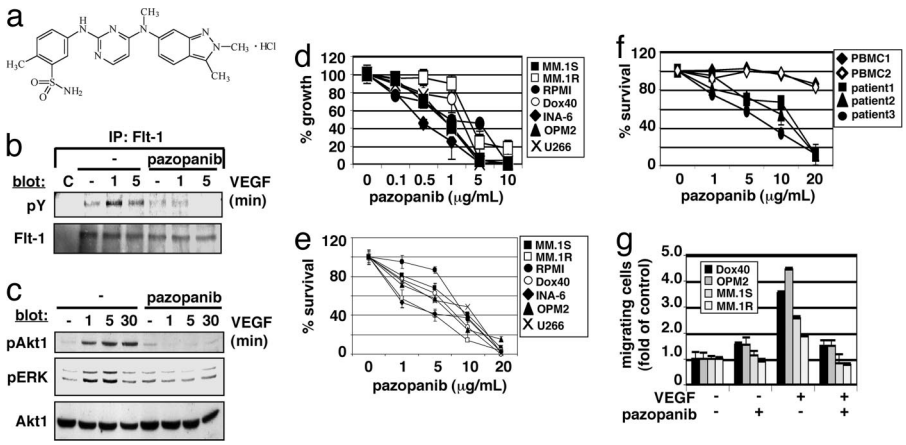

Fig. 1. Pazopanib inhibits MM cell growth, survival, and migration via VEGF-triggered Flt-1 phosphorylation and activation of downstream signaling molecules. (*a*) Chemical structure of pazopanib (GW786034B). (*b*) Pazopanib inhibits VEGF-induced Flt-1 autophosphorylation. (*c*) Pazopanib inhibits VEGF-induced phosphorylation of Akt1 and ERK. (*d*) Pazopanib induces inhibition of MM cell growth. Values represent mean ± SD ^{3}H[dT] uptake of triplicate cultures. (*e* and *f*) Pazopanib triggers MM cell cytotoxicity in MM cell lines (*e*) and CD138 plus patient cells, but not in normal PBMCs (*f*). MTT cleavage was measured during the last 4 h of a 48-h culture. Values represent the mean ± SD of quadruplicate cultures. (*g*) Pazopanib inhibits VEGF-triggered MM cell migration. Growth factor-deprived MM.1S, MM.1R, RPMI-Dox40 (Dox40), and OPM2 cells were pretreated with pazopanib or left untreated, plated on a fibronectin-coated polycarbonate membrane (8-μm pore size) in a modified Boyden chamber, and exposed to 10 ng/ml VEGF for 4 to 6 h.

a multicenter phase III trial in metastatic renal cell carcinoma (VEG105192) (www.clinicaltrials.gov).

Here, we show both *in vitro* and *in vivo* antitumor activity of pazopanib in MM. These preclinical data already have provided the framework for a multicenter phase I/II study with pazopanib alone in patients with relapsed or refractory MM (www.clinicaltrials.gov). Importantly, we also demonstrate synergistic cytotoxicity of low-dose pazopanib with conventional and novel therapeutics, strongly supporting its future clinical evaluation in combination regimens to increase efficacy, overcome drug resistance, reduce toxicity, and improve patient outcome.

Results

Pazopanib Selectively Inhibits VEGF-Triggered Flt-1-Phosphorylation and Activation of Downstream Signaling Molecules. Pazopanib (GW786034B) is a novel, orally available small-molecule inhibitor of human VEGF receptor -1, -2, and -3 (Fig. 1*a*) (‖, 8). We first tested whether pazopanib can abrogate VEGF-induced VEGF receptor-1 (Flt-1) tyrosine phosphorylation in MM cells. Pazopanib inhibited both VEGF-triggered Flt-1 tyrosine phosphorylation (1 and 5 min) (Fig. 1*b*) and activation of downstream signaling molecules (Akt-1 and ERK for 1, 5, and 30 min) (10 μg/ml for 1 h) (Fig. 1*c*). Taken together, these data show that pazopanib inhibits VEGF-triggered pathways in MM cells.

Pazopanib Inhibits MM Cell Growth, Survival, and Migration. The impact of pazopanib on MM cell growth, survival, and migration was investigated next. Our data show that pazopanib decreased growth (Fig. 1*d*) and survival (Fig. 1*e*) in all MM cell lines tested, including dexamethasone-sensitive MM.1S, dexamethasone-resistant MM.1R, doxorubicin (Dox)-sensitive RPMI, Dox-resistant RPMI (Dox40), IL-6-dependent INA-6, OPM2, and U266. Decreased survival consistently was observed with an IC_{50} ranging between 5 and 15 μg/ml pazopanib. Similar IC_{50} values were obtained in cells derived from three MM patients. In contrast, survival of PBMCs derived from normal donors was affected only slightly at high concentrations of pazopanib, thereby suggesting a large therapeutic window (Fig. 1*f*). Pazopanib also inhibited VEGF-triggered MM cell migration in several MM cell lines (Fig. 1*g*). These data demonstrate that pazopanib inhibits MM cell growth, survival, and migration in both cell lines and patient cells.

Pazopanib Suppresses VEGF-Induced Endothelial Cell Proliferation and Migration. Increased microvessel density in MM patient BM specimens correlates with disease progression and poor prognosis (10, 11). VEGF is an essential regulator of physiologic endothelial cell growth, permeability, and migration *in vitro* and *in vivo*. VEGF-triggered activation of ERK and phosphatidylinositol 3-kinase in endothelial cells is predominantly initiated by *VEGFR-2* (*KDR*) autophosphorylation. We next tested whether pazopanib has direct effects not only on MM cells, but also on VEGF-induced signaling in endothelial cells. Our results show that pazopanib blocks both VEGF-triggered autophosphorylation of KDR (Fig. 2*a*) and downstream activation of ERK and Akt1 (Fig. 2*b*), thereby inhibiting proliferation of endothelial cells (Fig. 2*c*). During angiogenesis, activated endothelial cells form cellular networks starting with migration and alignment, followed by the development of capillary tubes and the sprouting of new capillaries. As shown in Fig. 2*d*, VEGF-triggered endothelial cell migration was blocked in a concentration-dependent manner by pazopanib. To evaluate tube formation by endothelial cells, we seeded human umbilical endothelial cells (HUVECs) and endothelial cells isolated from BM aspirates (MM ECs) on matrigel. The addition of VEGF enhanced human umbilical endothelial tubule formation in the control cultures, confirming its specific effects. Importantly, pazopanib blocked tubule formation in a dose-dependent manner (Fig. 2*e*). Taken together, these results demonstrate that pazopanib inhibits VEGF-triggered endothelial cell growth, survival, migration, and tubule formation.

Pazopanib Blocks VEGF-Induced Up-Regulation of Adhesion Molecules on Endothelial and MM Cells and MM Cell Proliferation in a Coculture System. Although the role of BM stromal cell and MM cell interaction conferring growth, survival, and drug resistance is well established, whether there is any interaction between endothelial cells and MM cells and its potential relevance in MM pathogenesis is unknown. Given the importance of VEGF in triggering MM cell growth and migration and its pivotal role in angiogenesis, endothelial cells may exert a previously unrecognized role in MM. Therefore, we next examined whether MM cell proliferation is influenced by the presence of endothelial cells. As shown in Fig. 3*a*, MM cell adhesion to endothelial cells up-regulates cell proliferation (≈2-fold), which is markedly inhibited at pazopanib concentrations >1 μg/ml. Of great interest are the mechanisms mediating this effect. VEGF up-regulates cell adhesion molecules ICAM-1 and

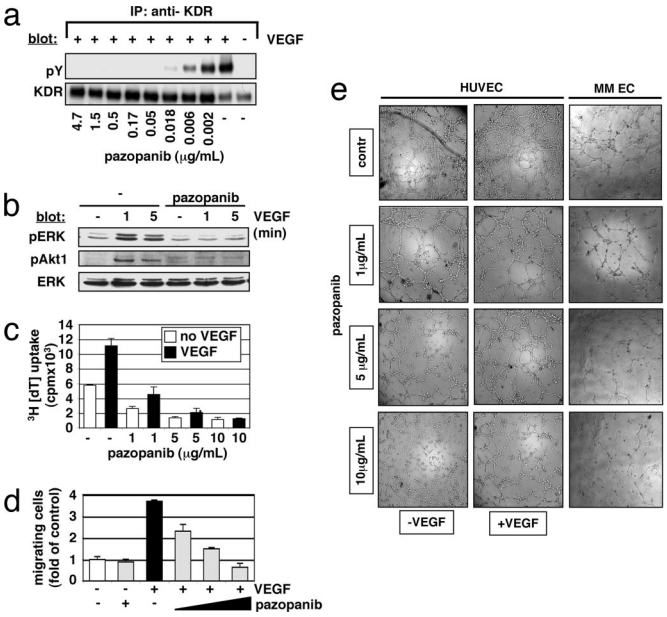

Fig. 2. Effects of pazopanib on endothelial cells. (*a* and *b*) Pazopanib inhibits VEGF-induced phosphorylation of KDR (*a*) and downstream activation of signaling molecules (*b*). (*c*) Pazopanib inhibits VEGF-triggered HUVEC proliferation. Values represent the mean ± SD ^{3}H[dT] uptake of triplicate cultures. (*d*) Pazopanib inhibits VEGF-triggered HUVEC migration. Growth factor-deprived HUVECs were pretreated with pazopanib (1, 5, and 10 μg/ml) or were left untreated. Cells then were placed on a polycarbonate membrane (8-μm pore size) in a modified Boyden chamber and were exposed for 6–10 h to 10 ng/ml VEGF. At the end of treatment, cells on the lower part of the membrane were counted by using a Coulter counter ZBII. Data represent mean ± SD for duplicate samples and are representative of three independent experiments. (*e*) Pazopanib inhibits VEGF-triggered endothelial tubule formation. HUVEC suspensions (with or without VEGF) or endothelial cells isolated from BM aspirates (MM EC) were premixed with different concentrations of pazopanib and added on top of the ECMatrix. Tube formation was assessed by using an inverted light microscope at ×4 and ×10 magnification. Photographs are representative of each group and three independent experiments.

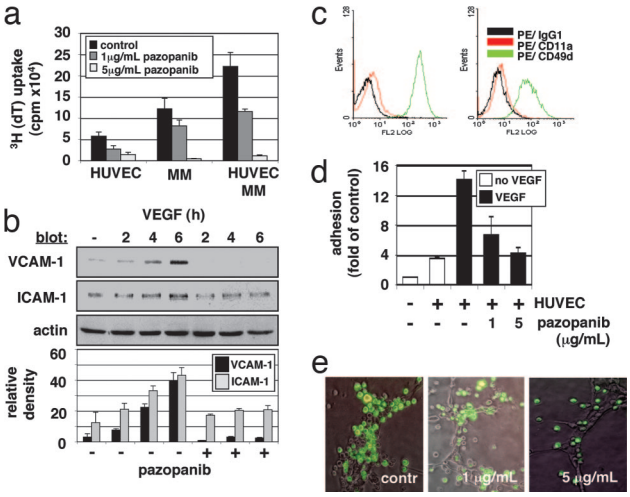

Fig. 3. Effect of pazopanib on endothelial-MM coculture systems. (a) Pazopanib inhibits proliferation of MM cells adherent to HUVECs. Data shown are mean ± SD of experiments performed in triplicate. (*b*) Pazopanib induces inhibition of VEGF-mediated up-regulation of surface adhesion proteins VCAM-1 and ICAM-1. Densitometry was used to quantitate expression data of three separate experiments. (*c*) Pazopanib triggers down-regulation of MM adhesion proteins. Control (*c Left*) MM.1S cells treated with pazopanib (5 μg/ml) (*c Right*) were examined for LFA-1 (CD11a/CD18) and VLA-4 (CD49d/CD29) expression by using immunofluorescence flow cytometric analysis. (*d*) Pazopanib induces dose-dependent inhibition of VEGF-induced MM cell adhesion on HUVECs. (*e*) Pazopanib decreases adhesion of MM cells in the branching points of endothelial tubule. HUVECs were cultured onto matrigel in EGM-2 medium supplemented with 2% FBS. After formation of tubules, MM/EGFP cells were added with or without pazopanib (1 and 5 μg/ml) for 6–10 h. After removing nonadherent cells, photographs of HUVECs were overlaid with photographs of MM/EGFP cells. Representative photographs (×10 magnification) of each group are shown.

VCAM-1 (12), and our data show that pazopanib specifically blocks this up-regulation (Fig. 3*b*). Pazopanib also down-regulates expression of very late antigen 4 (VLA-4, CD49d/CD29, or integrin $\alpha 4\beta 1$) and lymphocyte function-associated antigen-1 (LFA-1, CD11a/CD18, or integrin $\alpha L\beta 2$) on MM cells (Fig. 3*c*). Consequently, pazopanib quantitatively decreases adhesion of MM tumor cells to endothelial cells in an *in vitro* adhesion assay by using calcein-AM (Fig. 3*d*). Moreover, attachment of EGFP/MM cells to endothelial tubules is significantly decreased in the area of vascular branching points (Fig. 3*e*). These data therefore show that endothelial cells promote tumor cell growth via direct cell-cell contact and, conversely, that pazopanib specifically inhibits these effects.

Pazopanib Prolongs Survival in a Xenograft Mouse Model by Induction of Tumor Cell Apoptosis and Inhibition of Tumor Angiogenesis. Previous studies using first-generation small-molecule VEGF receptor inhibitors showed significant anti-MM activity *in vitro*; however, they failed to inhibit MM tumor growth *in vivo*. Having demonstrated effects of pazopanib on both MM cells and endothelial cells *in vitro*, we next sought to assess the *in vivo* efficacy of pazopanib by using a MM xenograft mouse model. Previous pharmacokinetic studies of pazopanib in xenograft models have shown tolerability without any significant side effects (13). Immune-deficient beige-nude-xid (BNX) mice were inoculated s.c. in the flank with 3×10^7 MM.1S cells. When the tumors reached a palpable size, mice were randomized into two treatment groups (30 mg/kg and 100 mg/kg) and one control group. Pazopanib was administered daily by oral gavage over a five-week period. Tumor growth in treated mice was significantly delayed (30 mg/kg) or almost totally inhibited (100 mg/kg) compared with the control group (Fig. 4*a*). However, tumors rapidly regrew after cessation of treatment at day 30. Using Kaplan–Meier and log-rank analysis, the mean overall survival (OS) was 20 days [95% confidence interval, 18–23 days] in the control cohort versus 41 days (95% confidence interval, 34–49 days) and 51 days (95% confidence interval, 46–56 days) in groups treated with 30 mg/kg and 100 mg/kg pazopanib, respectively (Fig. 4*b*). Statistically significant prolongation in mean OS compared with control mice was observed in animals treated with 30 mg/kg ($P = 0.0016$) and 100 mg/kg ($P = 0.0007$). Importantly, treatment with either the vehicle alone or pazopanib did not affect body weight (Fig. 4*c*). Large areas of cells with condensed nuclei were seen in H&E stains of pazopanib-treated tumors, consistent with tumor cell apoptosis or necrosis (Fig. 4*d*). Consistent with these data, TUNEL assays on tumor sections from treated versus control mice showed significantly increased apoptosis (Fig. 4*e*). Finally, angiogenesis was reduced markedly within tumors of pazopanib-treated versus nontreated mice, as evidenced by CD31 staining (Fig. 4*f*). Taken together, these results demonstrate *in vivo* inhibition of tumor growth, increased MM cell apoptosis, and decreased angiogenesis, associated with prolongation of survival.

Synergistic Effects of Pazopanib with Conventional and Novel Therapies in a Tumor Cell-Endothelial Cell Coculture. Given the discrepancy between the marked antitumor activity of antiangiogenic inhibitors (e.g., VEGF receptor inhibitors) in animal models and the disappointing clinical results when these agents are used alone, ongoing trials are evaluating these agents with combination chemotherapy (6). *In vitro* combination experiments in MM historically have proven to be highly predictive of their therapeutic value in

Table 1. Synergistic effects of pazobanib with conventional and novel therapies in a tumor cell-endothelial cell coculture

Sample	Pazopanib	Fa	CI
1	1	0.7018	0.222
2	1	0.774	0.284
3	2.5	0.714	0.398
4	2.5	0.734	0.539
5	1	0.69	0.969
6	1	0.9089	0.483
7	2.5	0.96	0.122
8	2.5	0.98	0.128
9	1	0.6084	0.403
10	1	0.6925	0.458
11	2.5	0.617	0.776
12	2.5	0.722	0.558

Pazopanib sensitizes MM cells bound to endothelial cells to immunomodulatory drugs (lenalidomide and actimid, respectively; samples 1–4), bortezomib (samples 5–8), and low-dose DNA-damaging agents like melphalan (samples 9–12). MM.1S-endothelial cell cocultures were treated or left untreated with pazopanib (1 and 2.5 μg/ml). Lenalidomide [0.5 μM (samples 1 and 3) and 2 μM (samples 2 and 4)], bortezomib [2.5 nM (samples 5 and 7) and 5 nM (samples 6 and 8)], and melphalan [0.5 μM (samples 9 and 11) and 2 μM (samples 10 and 12)] were added for 48 h. Proliferation was measured by using ^{3}H[dT] uptake. Fa, fraction of cells with growth affected in drug-treated versus untreated cells. CI, combination index. CI values <1 indicate synergism.

patients. For example, based on our preclinical data, cotreatment regimens such as thalidomide and dexamethasone (14) and bortezomib and dexamethasone (15) already have been translated successfully into the clinical setting by our own and other groups (16). We therefore next sought to assess the impact of combinations of pazopanib with novel and conventional therapies in MM cell-endothelial cell cocultures. Isobologram analysis demonstrates that combination regimens of pazopanib with immunomodulatory drug (IMiDs) such as lenalidomide (Table 1) and actimid (data not shown), bortezomib, and melphalan induce synergistic cytotoxicity [combination index (CI) <1]. Interestingly, inhibition of caspase-8 (IETD-FMK) significantly decreased pazopanib-triggered MM cell death, whereas inhibition of caspase-9 (LEHD-FMK) had only a moderate effect (data not shown). Bortezomib triggers both caspase-8- and caspase-9-mediated MM cell death (17). Furthermore, bortezomib, like thalidomide and the immunomodulatory drugs, also inhibits endothelial cell growth. Taken together, these data demonstrate the synergistic effect of low-dose pazopanib with conventional and novel therapeutics, providing the framework for combination clinical trials to increase efficacy, overcome drug resistance, and reduce toxicity.

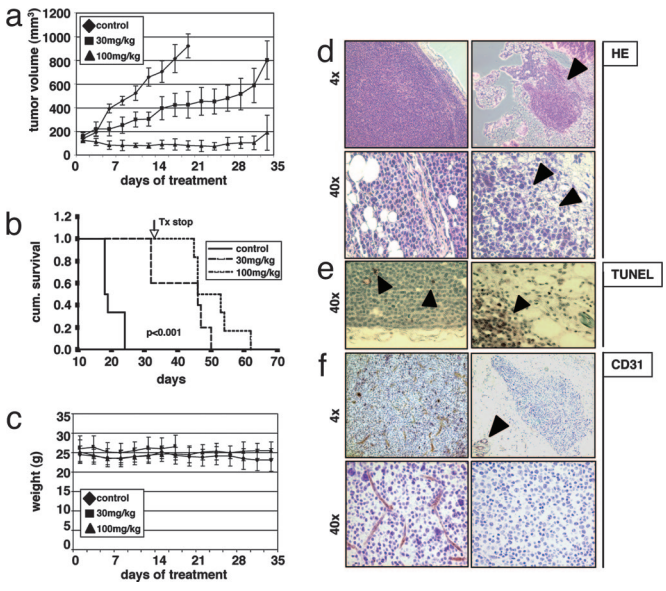

Fig. 4. Pazopanib prolongs survival in a xenograft mouse model by induction of tumor cell apoptosis and inhibition of tumor angiogenesis. Beige-nude Xid mice were inoculated s.c. with 3×10^7 MM.1S MM cells. Daily treatment by oral gavage (vehicle alone, 30 mg/kg, and 100 mg/kg) was started when tumors were measurable. (*a*) Tumor burden was measured every other day by using a caliper [calculated volume = $(4\pi / 3) \times (\text{width} / 2)^2 \times (\text{length} / 2)$]. Tumor volume is presented as means ± SE. (*b*) Survival was evaluated by using Kaplan–Meier curves and log-rank analysis. (*c*) Body weight was evaluated 3 times a week. (*d–f*) Representative microscopic images of tumor sections are shown stained with hematoxylin/eosin (HE) (*d*), TUNEL (*e*), and anti-CD31 (*f*).

Pazopanib-Triggered Transcriptional Changes. To further delineate pazopanib-targeted molecular pathways in MM cells, we performed gene expression profiling of MM cells treated with pazopanib (5 μg/ml for 2, 6, and 12 h) versus control cells (2, 6, and 12 h). Early (2 h) dysregulation of several cancer-relevant genes and pathways was evident. For example, interleukin and chemokine receptors, several members of the TGF-β pathway, cyclins, and genes belonging to the ubiquitin and the insulin-receptor pathways were modulated. In addition, gene ontology analysis by using MappFINDER (18) [supporting information (SI) Fig. 5*a*] demonstrated significant up-regulation of genes within the proapoptotic gene ontology group, including BCL2L11, BBC3 (PUMA), PMAIP1 (NOXA), BNIPL3, and Caspase-1, and significant down-regulation of genes within the mitosis control pathway, including BUB1B, Aurora kinase A, Separin, Wee1, and CDC25A. Interestingly, Kops *et al.* (19) recently demonstrated that down-regulation of BUB1B leads to inhibition of the mitotic checkpoint, thereby inducing apoptosis in human cancer cells through massive chromosomal loss. Ongoing studies are evaluating the role of BUB1B in MM pathogenesis.

Furthermore, several gene products associated with MM pathogenesis including MMSET, Maf, and Syndecan 1 (CD138 and SDC1) were reduced markedly in pazopanib-treated MM cells. c-Myc was the gene most down-regulated compared with control (>30 fold reduction at 2 h, with further down-regulation at subsequent time points) (SI Fig. 5 *a* and *b*).

At later time points, other cancer-relevant genes and pathways were dysregulated, including down-regulation of survivin, Mcl-1, caveolin-1 (SI Fig. 5*c*), IL6 receptor, insulin-like growth factor 1 receptor, intergrins β7 and α4 (data not shown), and up-regulation of p21 (SI Fig. 5*c*).

Deletion of c-Myc Results in Decreased Production and Secretion of VEGF. Our results identified transcriptional changes of several cancer-related genes and signaling pathways. Specifically, c-Myc showed the most dramatic reduction in expression after pazopanib treatment. Based on these findings, we sought to identify possible functional sequelae of c-Myc down-regulation. Specifically, recent reports have demonstrated that c-Myc regulates VEGF production in B cells, identifying VEGF as a mediator of c-Myc-induced angiogenesis (20–22). We therefore tested whether c-Myc plays a major role on VEGF production and angiogenesis also in MM cells.

To identify the specific functional impact of c-Myc inhibition on VEGF production and secretion, we transiently transfected MM.1S cells with c-Myc siRNA. As shown in SI Fig. 6*a*, c-Myc protein expression was down-regulated significantly by transfection with c-Myc, but not control, siRNA. We observed a decrease in mRNA levels of $VEGF_{145}$ and $VEGF_{165}$, but not $VEGF_{121}$ (23) (SI Fig. 6*b*), and a decrease of VEGF secretion (SI Fig. 6*c*) in c-Myc-depleted cells. Besides these results showing the requirement of c-Myc for autocrine VEGF secretion by MM cells, our data also demonstrate that targeted c-Myc down-regulation inhibits proliferation of both MM cells alone and cell proliferation in endothelial cell-MM cell

MEDICAL SCIENCES

cocultures (SI Fig. 6*d*). Similarly, pazopanib down-regulates VEGF mRNA levels after 12 h (SI Fig. 6*e*), as observed in siRNA transfectants. Taken together, these data show that pazopanib inhibits c-Myc in MM cells, thereby decreasing VEGF production and secretion.

Discussion

The BM microenvironment is comprised of a heterogeneous population of cells promoting growth, survival, and drug resistance of MM cells due to both direct cell-to-cell contact and cell-to-extracellular-matrix contact and by growth factors and chemokines secreted by tumor cells, stromal cells, and distant nonhematopoietic organs (3). Increased levels of VEGF are present in the BM of MM patients with progressive disease and associated with increased angiogenesis (10, 11). Preclinical studies show that VEGF directly triggers MM cell growth, migration, and survival, increases osteoclast activity and chemotaxis, and inhibits dendritic cell maturation, thereby potentially contributing to the clinical features of MM, including lytic bone lesions and immune deficiency (3). We and others therefore suggested that direct and/or indirect targeting of VEGF and its receptors may provide a potent therapeutic approach in the treatment for this incurable disease.

Because of acceptable tolerability and preliminary evidence of clinical activity in solid tumors (9), we here characterized the effect of the novel, orally available, small-molecule VEGF receptor inhibitor pazopanib on MM cell growth in the BM milieu. Specifically, our data demonstrate that pazopanib inhibits tumor cell growth, survival, and migration as well as endothelial cell growth, migration, and vessel formation. Moreover, we identify a role of endothelial cell-tumor cell binding in promoting MM cell proliferation that, at least in part, is mediated via VEGF-triggered up-regulation of integrins. Pazopanib, by decreasing expression of integrins on both MM cells and endothelial cells, abrogates MM cell adhesion to endothelial cells, thereby inhibiting MM cell proliferation. VEGF-triggered effects in MM cells are mediated predominantly via VEGF-R1 and, in endothelial cells, predominantly via VEGF-R2. However, it is possible that pazopanib, similar to imatinib mesylate and the novel Abl inhibitors AMN107 and BMS354825, also targets other tyrosine kinases. Indeed, inhibition of PDGF receptor α and β and c-*Kit* activity has been observed with pazopanib, although at IC_{50} values significantly higher than those for inhibition of VEGF receptors (‖, 13). However, to define potential off-site targets of pazopanib in detail, we are initiating comparative *in vivo* studies of pazopanib and VEGF-blocking antibodies, e.g., DC101 (ImClone), B20-4, and G6 (Genentech) (24, 25).

Importantly, pazopanib is a VEGF receptor inhibitor, which inhibits *in vivo* tumor growth, increases MM cell apoptosis, decreases angiogenesis, and prolongs host survival in a xenograft model of human MM. However, tumors regrew rapidly after treatment was stopped at day 30. The discrepancy between marked anti-tumor activity of antiangiogenic inhibitors (e.g., VEGF receptor inhibitors) in animal models versus the disappointing clinical results when used as single agents has resulted in their use with combination chemotherapy (6). Besides increasing the efficacy of chemotherapeutics, this strategy may (*i*) allow use of doses significantly below the maximum tolerated dose, thereby decreasing adverse side effects, and (*ii*) permit drug administration for prolonged uninterrupted periods, thereby preventing development of drug resistance or even overcoming drug resistance (26–28). Therefore, administration of VEGF receptor inhibitors in combination with other drugs may be required to achieve maximal efficacy. Specifically, our data demonstrate a synergistic effect of low-dose pazopanib with conventional and novel therapeutics, providing the basis for combination clinical trials to increase efficacy, overcome drug resistance, and reduce toxicity. Besides its use in combination with other chemotherapeutics, the clinical success of pazopanib likely will depend also on tumor stage and prior treatment (29–31).

Finally, further delineation of pazopanib-triggered effects in MM cells by using gene expression and signaling network analysis shows transcriptional changes of several cancer-related genes and signaling pathways, most significantly c-Myc. Using siRNA, we confirm the role of c-Myc in VEGF production and secretion and, thereby, angiogenesis in MM.

Based on these preclinical data, a multicenter phase I/II study with single agent pazopanib is ongoing in patients with relapsed or refractory MM. Importantly, our studies additionally demonstrate synergistic cytotoxicity of low-dose pazopanib with conventional and novel therapeutics, strongly supporting its future clinical evaluation in combination regimens to increase efficacy, overcome drug resistance, reduce toxicity, and improve patient outcome. Although the present study focuses only on the effects of pazopanib on tumor and endothelial cells, pazopanib also may abrogate other sequelae of VEGF within the MM BM microenvironment. Specifically, it may block VEGF stimulation of osteoclast activity and release VEGF-mediated suppression of dendritic cell maturation, with resultant clinical benefits of decreased bone disease and improved immune function.

Materials and Methods

Materials. Pazopanib (GW786034B), benzenesulfonamide,5-[4-[(2,3-dimethyl-2H-indazol-6-yl)methylamino]-2-pyrimidinyl]-amino]-2-methyl-monohydrochloride (M_r 474.0), was provided by GlaxoSmithKline. rhum $VEGF_{165}$ was obtained from R & D Systems (Minneapolis, MN), Abs were obtained from Santa Cruz Biotechnology (Santa Cruz, CA) and Cell Signaling Technology (Beverly, MA). The anti-phosphotyrosine 4G10 antibody was kindly provided by Tom Roberts (Dana–Farber Cancer Institute).

Cells and Cell Culture. All human MM cell lines and primary patient MM cells were cultured as described in ref. 23. HUVECs from a pool of five healthy donors (kindly provided by A. Cardoso and M. Tavares, Dana–Farber Cancer Institute) were maintained in EGM-2MV media (Cambrex BioScience, Walkersville, MD) containing 2% FBS. Isolation of endothelial cells from BM aspirates was performed as described in ref. 32.

Isolation of Patient's Tumor Cells. After appropriate informed consent, MM patient cells (96% CD38+CD45RA−) were obtained as described in ref. 23.

Cell Lysis, Immunoprecipitation, and Western Blotting. Cell lysis, immunoprecipitations, and Western blot analysis were performed as described in ref. 23.

Transfections and Retroviral Transductions. For c-Myc-specific knockdown experiments, MM.1S cells were transfected transiently with indicated amounts of siRNA SMARTpool c-Myc or nonspecific control duplexes (pool of four) by using the Cell Line Nucleofector Kit V Solution (Amaxa Biosystems, Cologne, Germany). Lentiviral transduction of MM.1S cells by using pHAGE-CMV-GFP-W lentiviral vector (kind gift of G. Mostoslavsky and R. C. Mulligan, Children's Hospital, Boston, MA) was performed as described in ref. 33. EGFP-positive cells were isolated by FACS after 20 h.

Transwell Migration Assay. Cell migration was assayed by using a modified Boyden chamber assay as described in ref. 23.

DNA Synthesis and Cell Proliferation Assay. Cell growth was assessed by measuring [^{3}H]thymidine uptake as described in ref. 23.

Microarray Assay. Total RNA was isolated from pazopanib pretreated or untreated MM.1S cells by using TRIzol reagent (Invitrogen, Carlsbad, CA). U133A 2.0 arrays were hybridized with biotinylated *in vitro* transcription products (10 μg per chip), as per

manufacturer's instructions, within the Dana–Farber Cancer Institute Microarray Core Facility and then analyzed by using a Gene Array Scanner (Affymetrix). CEL files were obtained by using Affymetrix Microarray Suite 5.0 software. The DNA Chip Analyzer (34) was used to normalize all CEL files to a baseline array with overall median intensity, and the model-based expression (perfect match minus mismatch) was used to compute the expression values. Probes showing at least 1.5-fold difference between control and pazopanib-treated cells at 2, 6, and 12 h were included in the analysis. The average fold change at the three time points was used for the analysis by using GenMAPP (35). Gene ontology analysis was performed by using MappFINDER (18). A Z score >2 was considered significant (18). The same data also were analyzed through the use of Ingenuity Pathways Analysis (Ingenuity Systems). Cell viability, as assessed by trypan blue exclusion, was $>85\%$ in all pazopanib-treated cells during times indicated.

Reverse Transcription PCR Analysis of VEGF. Total RNA was prepared with TRIzol reagent according to the manufacturer's instructions. Complementary DNA (cDNA) was synthesized by means of SuperScript One-Step RT-PCR system, as described in ref. 23. The integrity of messenger RNA of all samples was confirmed by amplification of GAPDH. PCR products were separated on a 1% agarose gel and photographed.

ELISA. Cyokine levels were measured in supernatants from coculture systems as described in ref. 23.

***In Vitro* Angiogenesis Assay.** The antiangiogenic potential of pazopanib was studied by using an *in vitro* angiogenesis assay kit (Chemicon, Temecula, CA) as per manufacturer's instructions. Tube formation was assessed by using an inverted light/fluorescence microscope at $\times 4$–$\times 10$ magnification.

FACS Analysis. MM.1S cells were cultured for 6 h in the presence or absence of pazopanib, washed, and then stained with specific Abs directed against CD11a (LFA-1) and CD49d (VLA-4) (BD Biosciences Pharmingen, San Diego, CA) and analyzed by using indirect immunofluorescence assays and flow cytometric analysis.

Cell Adhesion Assays. Adhesion assays were performed by using the Vybrant Cell Adhesion Assay Kit (Molecular Probes, Eugene, OR) as described in ref. 36. All experiments were done in triplicate.

MM Xenograft Mouse Model. To determine the *in vivo* anti-MM activity of pazopanib, mice were inoculated s.c. in the right flank with 3×10^7 MM.1S MM cells in 100 μl of RPMI medium1640, together with 100 μl of Matrigel (Becton Dickinson Biosciences, Bedford, MA). When the tumor was measurable, mice were assigned to indicated pazopanib treatment groups or a control group. Pazopanib was suspended in 0.5% hydroxypropylmethyl cellulose (Sigma-Aldrich, St. Louis, MO) and 0.1% Tween-80 (Sigma-Aldrich) in water as a vehicle (pH 1.3–1.5) and given daily by oral gavage for indicated periods (37). The control group received the carrier alone at the same schedule and route of administration. Tumor burden was measured every other day by using a caliper [calculated volume $= (4\pi / 3) \times (\text{width} / 2)^2 \times (\text{length} / 2)$]. Animals were killed when their tumor reached 2 cm or when the mice became moribund. Survival was evaluated from the first day of treatment until death (38).

Immunohistochemistry. Four-micrometer-thick sections of formalin-fixed tissue were used for TUNEL staining and staining with CD31 Ab (Becton Dickinson Pharmingen) in a humid chamber at room temperature, as in ref. 38. For image capturing, the Leica DM IRB microscope was connected to an Optimetrics camera and exported to MagnaFire software.

Isobologram Analysis. For combination studies, data from ^{3}H[dT] uptake assays were converted into values representing the fraction of growth affected in drug-treated versus untreated cells and analyzed by using the CalcuSyn software program (Biosoft, Ferguson, MO) based on the Chou–Talalay method. A combination index <1 indicates synergism, whereas 1 indicates additive effects.

Statistical Analysis. Statistical significance of differences observed in VEGF-treated versus control cultures was determined by using an unpaired Student's t test. The minimal level of significance was $P < 0.05$. Overall survival in animal studies was measured by using the Kaplan–Meier method, and results are presented as the median overall survival, with 95% confidence intervals.

We thank M. Simoncini, F. Abtahi, and J. Zhang for technical assistance; Dr. R. T. Bronson (Rodent Histopathology Core, Harvard Medical School), M. Zheng, and D. Geer for mouse histopathological studies; Drs. J. Folkman (Children's Hospital, Harvard Medical School), A. Vacca (University of Bari Medical School), R. D. Carrasco, and L. Catley (Dana–Farber Cancer Institute) for helpful discussions; and Drs. P. G. Richardson and R. Schlossman and the patients, nursing staff, and clinical research coordinators of the Jerome Lipper Multiple Myeloma Center (Dana–Farber Cancer Institute) for their help in providing primary tumor specimens for this study. This work was supported by National Institutes of Health Grants R01 CA50947, P01 CA78378, and P50 CA100707 and the Doris Duke Distinguished Clinical Research Scientist Award (to K.C.A.).

1. Folkman J (1971) *N Engl J Med* 285:1182–1186.
2. Folkman J (2001) *Semin Oncol* 28:536–542.
3. Podar K, Anderson KC (2005) *Blood* 105:1383–1395.
4. Ferrara N, Gerber HP, LeCouter J (2003) *Nat Med* 9:669–676.
5. Kyle RA, Rajkumar SV (2004) *N Engl J Med* 351:1860–1873.
6. Ferrara N, Hillan KJ, Gerber HP, Novotny W (2004) *Nat Rev Drug Discov* 3:391–400.
7. Marx J (2005) *Science* 308:1248–1249.
8. GlaxoSmithKline (2006) *Pharmacopeial Forum* 32:217.
9. Hurwitz H, Dowlati A, Savage S, Fernando N, Lasalvia S, Whitehead B, Suttle B, Collins D, Ho P, Pandite L (2005) *J Clin Oncol* 23:1955.
10. Vacca A, Ribatti D, Roncali L, Ranieri G, Serio G, Silvestris F, Dammacco F (1994) *Br J Haematol* 87:503–508.
11. Vacca A, Ribatti D, Presta M, Minischetti M, Iurlaro M, Ria R, Albini A, Bussolino F, Dammacco F (1999) *Blood* 93:3064–3073.
12. Kim W, Moon SO, Lee S, Sung MJ, Kim SH, Park SK (2003) *Arterioscler Thromb Vasc Biol* 23:1377–1383.
13. Kumar R, Harrington LE, Hopper TM, Miller CG, Onori JA, Cheung M, Stafford JA, Epperly AH, Gilmer TM (2005) *J Clin Oncol* 23:9537.
14. Hideshima T, Chauhan D, Shima Y, Raje N, Davies FE, Tai YT, Treon SP, Lin B, Schlossman RL, Richardson P, *et al.* (2000) *Blood* 96:2943–2950.
15. Hideshima T, Richardson P, Chauhan D, Palombella VJ, Elliott PJ, Adams J, Anderson KC (2001) *Cancer Res* 61:3071–3076.
16. Rajkumar SV (2005) *Oncology (Williston Park)* 19:621–625.
17. Hideshima T, Bergsagel PL, Kuehl WM, Anderson KC (2004) *Blood* 104:607–618.
18. Doniger SW, Salomonis N, Dahlquist KD, Vranizan K, Lawlor SC, Conklin BR (2003) *Genome Biol* 4:R7.
19. Kops GJPL, Foltz DR, Cleveland DW (2004) *Proc Natl Acad Sci USA* 101:8699–8704.
20. Baudino TA, McKay C, Pendeville-Samain H, Nilsson JA, Maclean KH, White EL, Davis AC, Ihle JN, Cleveland JL (2002) *Genes Dev* 16:2530–2543.
21. Mezquita P, Parghi SS, Brandvold KA, Ruddell A (2005) *Oncogene* 24:889–901.
22. Knies-Bamforth UE, Fox SB, Poulsom R, Evan GI, Harris AL (2004) *Cancer Res* 64:6563–6570.
23. Podar K, Tai YT, Davies FE, Lentzsch S, Sattler M, Hideshima T, Lin BK, Gupta D, Shima Y, Chauhan D, *et al.* (2001) *Blood* 98:428–435.
24. Witte L, Hicklin DJ, Zhu Z, Pytowski B, Kotanides H, Rockwell P, Bohlen P (1998) *Cancer Metastasis Rev* 17:155–161.
25. Liang WC, Wu X, Peale FV, Lee CV, Meng YG, Gutierrez J, Fu L, Malik AK, Gerber HP, Ferrara N, Fuh G (2006) *J Biol Chem* 281:951–961.
26. Hanahan D, Bergers G, Bergsland E (2000) *J Clin Invest* 105:1045–1047.
27. Browder T, Butterfield CE, Kraling BM, Shi B, Marshall B, O'Reilly MS, Folkman J (2000) *Cancer Res* 60:1878–1886.
28. Kerbel RS, Kamen BA (2004) *Nat Rev Cancer* 4:423–436.
29. Miller KD (2003) *Clin Breast Cancer* 3:421–422.
30. Casanovas O, Hicklin DJ, Bergers G, Hanahan D (2005) *Cancer Cell* 8:299–309.
31. Bisping G, Kropff M, Wenning D, Dreyer B, Bessonov S, Hilberg F, Roth GJ, Munzert G, Stefanic M, Stelljes M, *et al.* (2006) *Blood* 107:2079–2089.
32. Roccaro AM, Hideshima T, Raje N, Kumar S, Ishitsuka K, Yasui H, Shiraishi N, Ribatti D, Nico B, Vacca A, *et al.* (2006) *Cancer Res* 66:184–191.
33. Podar K, Mostoslavsky G, Sattler M, Tai YT, Hayashi T, Catley LP, Hideshima T, Mulligan RC, Chauhan D, Anderson KC (2004) *J Biol Chem* 279:21658–21665.
34. Li C, Wong WH (2001) *Proc Natl Acad Sci USA* 98:31–36.
35. Dahlquist KD, Salomonis N, Vranizan K, Lawlor SC, Conklin BR (2002) *Nat Genet* 31:19–20.
36. Podar K, Tai YT, Lin BK, Narsimhan RP, Sattler M, Kijima T, Salgia R, Gupta D, Chauhan D, Anderson KC (2002) *J Biol Chem* 277:7875–7881.
37. Huh JI, Calvo A, Stafford J, Cheung M, Kumar R, Philp D, Kleinman HK, Green JE (2005) *Oncogene* 24:790–800.
38. Chauhan D, Catley L, Hideshima T, Li G, Leblanc R, Gupta D, Sattler M, Richardson P, Schlossman RL, Podar K, *et al.* (2002) *Blood* 100:2187–2194.